

# Wake state and energy transitions of an oscillating cylinder at low Reynolds number

J. S. Leontini,<sup>a)</sup> B. E. Stewart, M. C. Thompson, and K. Hourigan

*Fluids Laboratory for Aeronautical and Industrial Research (FLAIR),*

*Department of Mechanical Engineering, P. O. Box 31, Monash University, Melbourne, 3800, Australia*

(Received 20 December 2005; accepted 24 March 2006; published online 1 June 2006)

This paper reports on an extensive parameter space study of two-dimensional simulations of a circular cylinder forced to oscillate transverse to the free-stream. In particular, the extent of the primary synchronization region, and the wake modes and energy transfer between the body and the fluid are analyzed in some detail. The frequency range of the primary synchronization region is observed to be dependent on Reynolds number, as are the wake modes obtained. Energy transfer is primarily dependent on frequency at low amplitudes of oscillation, but primarily dependent on amplitude at high amplitudes of oscillation. However, the oscillation amplitude corresponding to zero energy transfer is found to be relatively insensitive to Reynolds number. It is also found that there is no discernible change to the wake structure when the energy transfer changes from positive to negative. © 2006 American Institute of Physics. [DOI: 10.1063/1.2204632]

## I. INTRODUCTION

A common approach to understanding vortex-induced vibration (VIV) has been to investigate the near wake and energy-transfer characteristics of a bluff body undergoing forced oscillation transverse to the free-stream (see reviews in Refs. 1 and 2). This approach provides an indication of flow regimes that may be produced by VIV and the expected amplitudes of oscillation. However, only limited fundamental research has been conducted to investigate the energy transfer for Reynolds number  $Re < 500$ , given  $Re = UD/\nu$ ,  $U$  is the freestream velocity,  $D$  is the cylinder diameter and  $\nu$  is the kinematic viscosity. Investigations at these lower Reynolds numbers are important for two reasons: first, interest in smaller scale flows is increasing, with applications such as biological systems and microvehicles becoming apparent; second, removing the complexity of spanwise variation that occurs at higher  $Re$  allows important flow features to be identified that may be critical in establishing causal links in behavior, even at higher  $Re$ . This is not to downplay the critical role of higher Reynolds number phenomena on VIV dynamics, such as the shear-layer instability, three-dimensionality, and formation length modification.

An extensive map of wake modes was generated by Williamson and Roshko<sup>3</sup> over the Reynolds number range  $300 < Re < 1000$ . In the region of primary synchronization (where the cylinder oscillation frequency,  $f$ , and the primary vortex-shedding frequency,  $f_V$ , are similar, i.e.,  $f_V \approx f$ ) two shedding modes were observed. These were the  $2S$  modes, with two single vortices per oscillation cycle, and the  $2P$  modes, consisting of two pairs of opposite-sign vortices shed per cycle. A third mode consisting of a pair and single vortex per oscillation cycle, the  $P+S$  mode, was discovered in this primary synchronization region at amplitudes of oscillation

$A^* > 1$ , where  $A^* = A/D$ ;  $A$  is the oscillation amplitude, and  $D$  is the cylinder diameter. An explanation for the multipaired modes has been offered by Govardhan and Williamson<sup>4</sup> that the pairs develop from a single vortex that becomes strained and splits in the near wake.

A recent paper from Ponta and Aref<sup>5</sup> presented a theoretical argument for the placement of boundaries on this wake map. Their theory matched the measurement of the circumferential-type boundaries well (for example, those defining the region of primary synchronization), but it was admitted that more assumptions were required to match the radial-type boundaries (those defining the transition between wake modes). It was suggested that the mechanism controlling the formation of different modes depended on a fine balance of the splitting mechanism discussed by Govardhan and Williamson.<sup>4</sup>

Energy transfer is defined as the work done on the cylinder by the fluid. It is quantified by the energy-transfer coefficient,  $C_E = \int_{\tau} C_L v d\tau$ , where  $v$  is the cylinder transverse velocity and  $\tau$  is nondimensionalized time,  $\tau = tUD$ . Carberry *et al.*<sup>6</sup> found experimentally that changes in the lift coefficient  $C_L$  of a cylinder undergoing forced oscillation were intrinsically linked to the formation of the near wake. Those results at a fixed amplitude of oscillation also show a discontinuity in the phase between the lift force and cylinder displacement as the frequency of oscillation  $f$  passes through a value close to  $f_{St}$ . Here,  $f_{St}$  is the shedding frequency from a fixed cylinder, corresponding to its Strouhal number. This phase “jump” was also used to infer a change in the sign of  $C_E$ . This discontinuity was first reported by Bishop and Hassan<sup>7</sup> and has since been observed at frequencies both above and below  $f_{St}$  at a range of Reynolds numbers.<sup>8–10</sup>

When the phase between cylinder displacement and lift force has been observed to jump through  $180^\circ$ , the sign of  $C_E$  changes from positive to negative or vice versa.<sup>3,6–8,11</sup> Hover *et al.*<sup>9</sup> produced contours of the lift coefficient in phase with transverse velocity,  $C_{L_V}$ , the component of lift that will con-

<sup>a)</sup> Author to whom correspondence should be addressed. Electronic mail: justin.leontini@eng.monash.edu.au; Phone: +61 3 9905 1573.

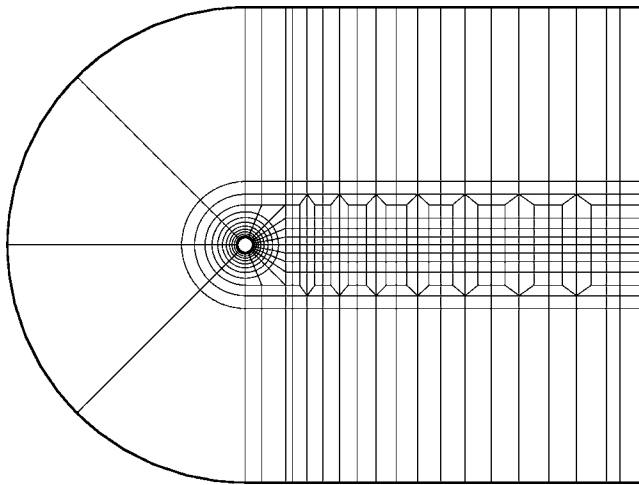


FIG. 1. The macroelement mesh used for the simulations.

tribute to  $C_E$ , at  $Re=3800$  and  $Re=10000$  in the amplitude-frequency plane. They found that the contour of  $C_{L_V}=0$  followed reasonably close to the data obtained from free vibration of a cylinder with low mechanical damping at  $Re=3800$ . This result showed that analysis of forced vibration is a useful tool for predicting the regions in which vortex-induced vibration is possible. Similar conclusions were drawn from the work of Staubli.<sup>12</sup> Driven oscillation can also be used to find a mechanism that directly influences the sign of energy transfer.

This study quantifies the energy transfer, using  $C_E$ . This has been undertaken for the region of primary synchronization in the frequency-amplitude plane. The effect of  $Re$  (over the two-dimensional shedding range) is also investigated by producing two maps of contours, one at  $Re=100$  and a second at  $Re=200$ . Two-dimensional simulations were used due to the two-dimensionality of this flow at these values of  $Re$ , even in experiments.<sup>13,14</sup>

The wake modes in this primary synchronization region have also been mapped. It is shown that the wake modes depend not only on the dimension of the problem, but also, when the flow is two-dimensional, on  $Re$ . It is also shown that the wake modes are not influenced by the value of  $C_E$ .

As the amplitude of oscillation is increased,  $C_E$  is seen to change sign from positive to negative. This phenomenon is explained in terms of the relative importance of different pressure regions in the flow near the cylinder.

## II. COMPUTATIONAL METHOD

The incompressible Navier-Stokes equations are solved in an accelerated frame of reference attached to the cylinder. To allow this, an extra (noninertial) forcing term is introduced into the momentum equation rendering the system to be solved as

$$\frac{\partial \mathbf{v}}{\partial \tau} = \nabla P + \frac{1}{Re} (\nabla^2 \mathbf{v}) - (\mathbf{v} \cdot \nabla) \mathbf{v} + \frac{d\mathbf{u}_F}{d\tau} \mathbf{j} \quad (1)$$

and

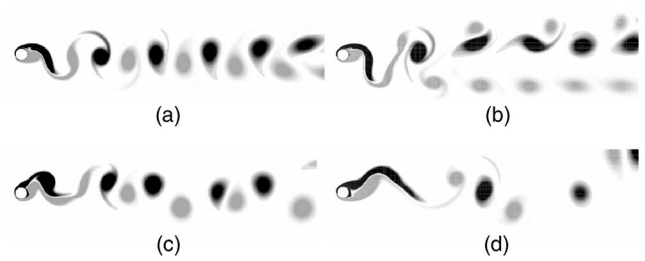


FIG. 2. (a) Synchronized 2S wake,  $A^*=0.4$ ,  $f/f_{St}=0.95$  ( $\lambda=5.3$ ). (b) Synchronized P+S wake,  $A^*=0.7$ ,  $f/f_{St}=0.95$  ( $\lambda=5.3$ ). (c) Short-wavelength 2S wake,  $A^*=0.4$ ,  $f/f_{St}=1.26$  ( $\lambda=4.0$ ). (d) Long-wavelength 2S wake,  $A^*=0.4$ ,  $f/f_{St}=0.68$  ( $\lambda=7.4$ ). All the images shown above are obtained for  $Re=200$ .

$$\nabla \cdot \mathbf{v} = 0, \quad (2)$$

where  $\mathbf{v}$  is the nondimensional velocity,  $\tau$  is nondimensional time,  $P$  is the kinematic pressure, and  $(d\mathbf{u}_F/d\tau)\mathbf{j}$  is the introduced noninertial forcing term, which is just the acceleration of the reference frame.

A three-step time-splitting scheme is employed in the solution of the velocity and pressure field. The three steps account for the advection, pressure and diffusion terms of the Navier-Stokes equation. The code has been validated to produce second-order time accuracy. Details of the time-splitting method can be found in Karniadakis *et al.*<sup>15</sup> and Thompson *et al.*<sup>16</sup>

A spectral-element technique is employed for the spatial discretization. The spatial domain is discretized into 508 elements, with the majority concentrated in the wake and boundary-layer regions. This macroelement mesh is shown in Fig. 1. This final mesh was chosen after an extensive mesh and domain optimization study. Within each element, the mesh geometry, as well as the velocity and pressure fields, are represented by eighth-order tensor-product polynomials, associated with Gauss-Lobatto-Legendre quadrature points. Details of overall approach and implementation have been provided elsewhere.<sup>16,17</sup> The base code has been validated extensively against experiments and other codes e.g., Refs. 18–21.

For the driven-oscillation problem, the cylinder position at any time is prescribed by the driving function. This allows the additional forcing term in the Navier-Stokes equations to be expressed explicitly.

Boundary conditions are set to  $u=U$  and  $v=-v_{cyl}$  at the inlet, top, and bottom boundaries, where  $u$  and  $v$  are the  $x$  and  $y$  velocity components, respectively, and  $v_{cyl}$  is the cylinder velocity in the absolute frame. At the cylinder wall, a no-slip condition is imposed. Higher-order boundary conditions<sup>15</sup> are used for the pressure gradient at no-slip boundaries and at the far-field boundaries. At the outlet, the pressure is fixed and the normal velocity gradient is set to zero.

## III. RESULTS

### A. Wake modes

One of the aims of this study is to identify the similarities and differences between the two-dimensional, and higher

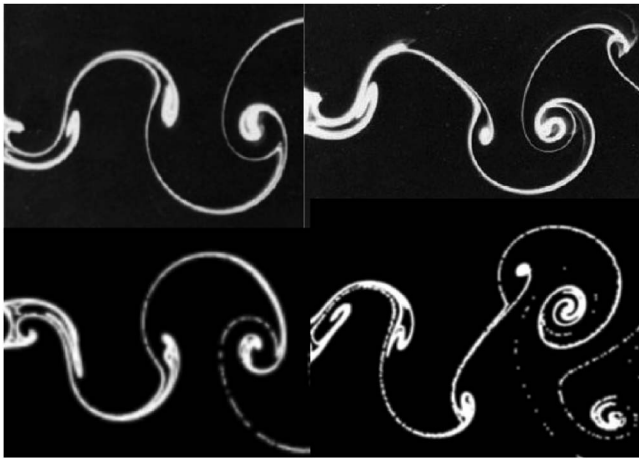


FIG. 3. Experimental dye visualizations from Williamson and Govardhan (Ref. 2) (top) and particle tracking visualization from the simulations (bottom). An close similarity between the two is clear.

Re three-dimensional flow. A logical starting point for this is to compare the wake mode topology obtained over the same parameter space. To facilitate this comparison, maps of wake modes have been produced at a series of values of Re using two-dimensional simulations.

In the region of primary synchronization, only two wake modes are observed, regardless of Re. At lower values of  $A^*$ , a synchronized  $2S$  shedding mode is observed, with two single vortices shed per oscillation cycle. An example of this mode is shown in Fig. 2(a). At higher values of  $A^*$ , a synchronized  $P+S$  shedding mode occurs, with one single and one pair of vortices of opposite sign shed per shedding cycle. This mode is shown in Fig. 2(b).

Outside the area of synchronization, variants of the  $2S$  mode are observed, referred to here as the short-wavelength and long-wavelength  $2S$  modes. Examples of these two modes are shown in Figs. 2(c) and 2(d). Comparison of Figs. 2(a) and 2(c) shows that the short wavelength  $2S$  mode is similar to the synchronized  $2S$  mode, except there is a longer period wandering about the wake centerline. This wandering appears to be due to beating between the cylinder oscillation

frequency and the fixed cylinder shedding frequency. The long wavelength  $2S$  wake represented in Fig. 2(d) shows no such interaction, and is more disordered.

The wake configurations obtained compare well with visualization taken from experiments at similarly low Reynolds numbers. Figure 3 shows dye visualizations taken from Williamson and Govardhan<sup>2</sup> compared with particle-tracking visualizations from simulations. It is clear that both the  $2S$  and  $P+S$  wake modes show a remarkable similarity to the experimental results. It should be noted that the  $P+S$  wake mode obtained appears very resilient, persisting all the way to the outflow boundary of the computational domain. Away from the synchronization boundaries, a periodic lift signal was reached within  $\approx 20$  periods of oscillation. Once this periodic signal was obtained, it persisted from thereon, with no loss of periodicity and no intermittency.

It is well known that the wake mode obtained at higher Re is dependent on the amplitude and frequency of oscillation, and this dependence is clear from observation of the wake mode map of Williamson and Roshko.<sup>3</sup> It has also been shown that a similar dependence occurs at lower values of Re, where the flow is two-dimensional (see the results of Ref. 22 also adapted in Ref. 2). However, an in-depth mapping of wake modes for the two-dimensional flow has not been produced. Also, the effect of Reynolds number has not previously been investigated separately.

These issues are addressed with the plots shown in Fig. 4. Figure 4(a) shows a wake-mode map, produced for Re=100. The Reynolds number was held constant over the entire  $A^*$ ,  $f/f_{St}$  parameter space, a luxury not often afforded in experiments. This wake map illustrates what has hitherto expected, but not quantified, for two-dimensional flow. First, it shows that only the  $2S$  and  $P+S$  wake modes are obtained in the region of primary synchronization. Secondly, it shows that the  $P+S$  wake mode occurs only in the region of the parameter space where  $C_E$  is negative, i.e., where there is energy transfer from the cylinder to the fluid. The contour of  $C_E=0$  is plotted ( $C_E < 0$  above this line), and the transition from  $2S$  to the  $P+S$  wake mode is shown to occur at values of  $A^*$  well above this.

However, some variations of these trends are seen for the

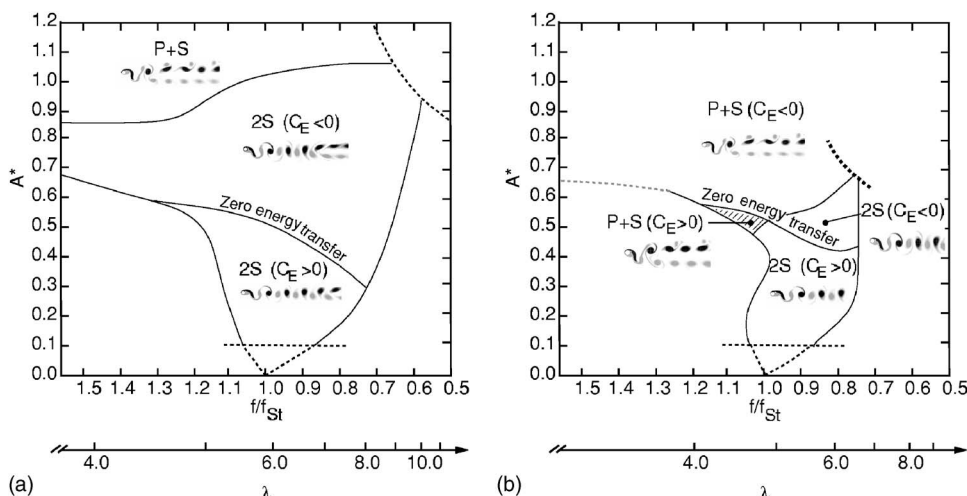


FIG. 4. Flow regimes for (a) Re=100 and (b) Re=300, in the primary synchronization region. It is clear that while the same wake modes are observed for both values of Re, there is an Re dependence on where the transitions between modes occur. It is also shown that at the higher value of Re = 300, a  $P+S$  wake configuration can be achieved along with a positive energy transfer ( $C_E > 0$ ) [see the hatched region of (b)].

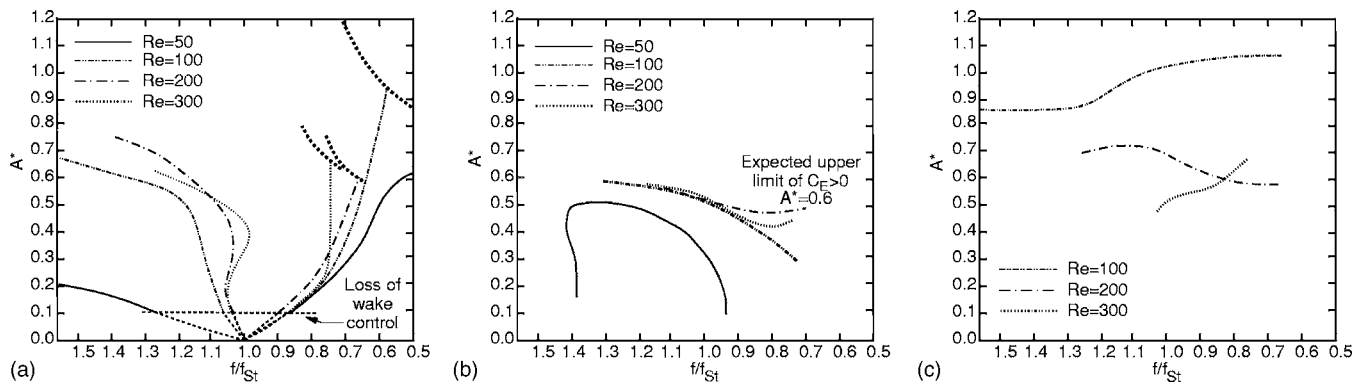


FIG. 5. (a) Synchronization boundaries, (b)  $C_E=0$ , and (c) the boundary defining the transition from the 2S to P+S wake mode for all values of Re tested. It can be deduced from (a) that the primary synchronization region widens with decreasing Re. From (b), it is clear that the upper limit for  $C_E > 0$  is approximately  $A^* = 0.6$ . The lines plotted in (c) show that the value of  $A^*$  at the transition from the 2S wake to the P+S wake is inversely varying with Re.

wake-mode map constructed at  $Re=300$ , shown in Fig. 4(b). Some of the trends observed at  $Re=100$  remain: only the 2S and P+S wake modes are observed in the primary synchronization region; and energy transfer becomes negative (from cylinder to fluid) at higher amplitudes. Two stark differences are clear though. The transition from the 2S to P+S wake mode occurs at much lower values of  $A^*$ , and the line defining this transition and the line defining  $C_E=0$  cross. This means that the P+S wake mode is observed with a positive energy transfer, where energy is transferred from the fluid to the cylinder. It has been suggested that this will not occur;<sup>2</sup> however, a similar finding to the one made here was made by Blackburn and Henderson<sup>8</sup> at  $Re=500$ . The current result is, to the authors' knowledge, the first demonstration that the phenomenon of a P+S wake mode with  $C_E > 0$  has been shown to be Re dependent. It is conceded that the value of  $Re=300$  at which it is observed is above the limit of two-dimensional flow for a fixed cylinder; although it has been reported that transverse oscillation can significantly defer the onset of three-dimensionality.<sup>13,23</sup> It therefore remains a point of conjecture as to whether this situation could be observed physically.

## B. Reynolds number dependence

Similar plots to Fig. 4 have been produced before for two-dimensional flow. However they have not included any information regarding the sign of  $C_E$ . They have also been produced at only one Reynolds number, whereas the inclusion of maps at different values of Re is a new contribution, and one that clearly demonstrates the Re dependence of the wake modes obtained in this flow.

As the results of the previous section have indicated, a strong Re dependence is present for the two-dimensional flows investigated. To investigate this, simulations have been performed at four different values of Re:  $Re=50$ , 100, 200, and 300. This allows a direct measure of the effect of Re and Re only. Three important transitions have been investigated in this manner: the boundaries of primary synchronization, the energy transfer quantified by  $C_E$ , and the transition from the 2S to P+S wake mode. All of these parameters are illustrated in plots in Fig. 5.

Figure 5(a) shows the boundaries of primary synchroni-

zation for all values of Re. A comparison of the low-frequency, long-wavelength synchronization boundary shows that Re has little effect on the position of that boundary at  $A^* < 0.20$ . At  $A^* > 0.20$ , it is shown that this boundary moves towards  $f/f_{St}=1$  with increasing Re.

A similar effect occurs with respect to the high-frequency short-wavelength synchronization boundary, with the synchronization region narrowing significantly with increasing Re. As well as this, the shape of this boundary changes with increasing Re: for the lower values of Re,  $Re=50$ , 100, the frequency at which synchronization is lost always increases with increasing  $A^*$ ; however, for  $Re=200$  and  $Re=300$ , the frequency at which synchronization is lost decreases with increasing  $A^*$  over the range  $0.2 \leq A^* \leq 0.4$ . This effect becomes more pronounced with increasing Re. This demonstrates that the amount that the wake oscillation can be shifted from its natural frequency is Re dependent, at least for Reynolds numbers where the flow is two-dimensional. Both these boundaries also show that at very low values of Re, synchronization can effectively be obtained for any frequency if a moderate amplitude of oscillation is used.

Figure 5(b) shows the contour  $C_E=0$  for all values of Re. It is shown that the amplitude at which  $C_E=0$  increases with increasing  $f/f_{St}$ . Only the lowest value of Re tested,  $Re=50$ , proceeded to turn over, and put an upper frequency limit on the region of  $C_E > 0$ . What should be taken from this plot is that at all values of Re, the highest amplitude at which  $C_E \geq 0$  is  $A^* \approx 0.6$ . This is important as it provides a prediction of the highest amplitudes of oscillation possible during vortex-induced vibration of elastically mounted cylinders in two-dimensional flow. This approximation fits well with the upper amplitudes obtained experimentally by Anagnostopolous and Bearman<sup>24</sup> and the simulations of Blackburn and Henderson,<sup>25</sup> and others (see the two-dimensional flow Griffin plot in Williamson and Govardhan<sup>2</sup> for these and many others).

Figure 5(c) shows the boundary defining the transition from the 2S to P+S wake modes for  $Re=100$ , 200, and 300. For all values of Re, the 2S wake is observed below this boundary, and the P+S mode is observed above it. The general trend shown is that the amplitude at which this transition

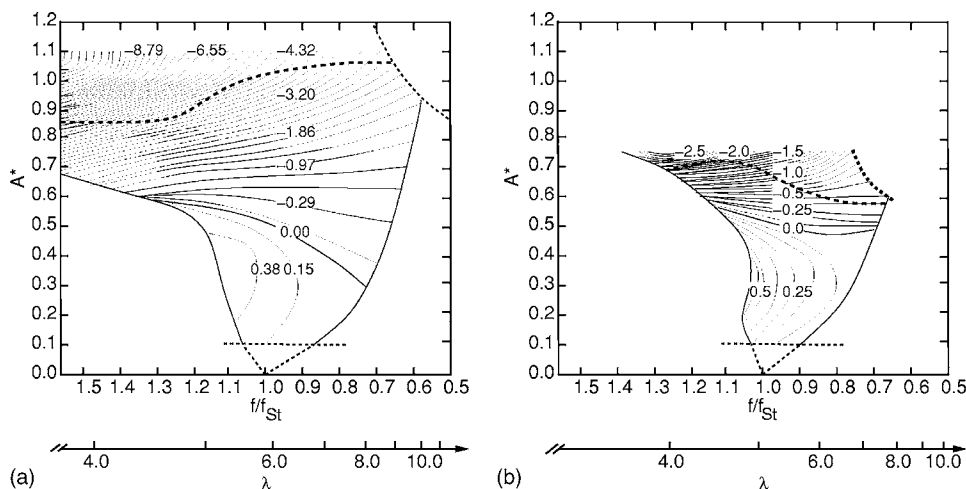


FIG. 6. Contours of the energy transfer coefficient,  $C_E$ , for (a)  $Re=100$  and (b)  $Re=200$ , in the primary synchronization region. Also marked is the boundary defined by the  $2S$  to  $P+S$  wake transition (---). These plots show that the transition from  $2S$  to  $P+S$  is not dependent on  $C_E$ . They also show the increasing effect of  $A^*$  on  $C_E$  with increasing  $A^*$ .

occurs decreases with increasing  $Re$ . Some frequency dependence is also observed but there is not a consistent trend. Why this occurs is still unclear. As this boundary appeared at higher values of  $A^*$  with decreasing  $Re$ , the  $P+S$  wake mode is not observed at  $Re=50$  for the range of  $A^*$  tested.

It is also interesting to consider this boundary in terms of the symmetries that occur on either side of it. The  $2S$  wake possesses a  $Z_2$  symmetry group.<sup>26</sup> This describes its spatio-temporal symmetry; if the flow is evolved forward in time by a half a period, and then reflected spatially about the wake centerline, the original wake pattern is recovered. This symmetry is lost after the transition to the  $P+S$  wake mode. For a given value of  $Re$ , when this transition occurs is primarily dependent on  $A^*$ . However, Fig. 5(c) shows that varying  $Re$  has a marked effect on this transition. Insight has been gained into transitions of fluid systems, particularly transitions to three-dimensionality, by analyzing the symmetry-breaking characteristics of their bifurcations. The systems analyzed are generally codimension-one, where there is effectively only one variable.<sup>27-29</sup> This system has more than one variable, allowing other possible generic bifurcation types. The experimental results of Williamson and Govardhan<sup>2</sup> reproduced in Fig. 3 show that the  $P+S$  wake is physical, and not simply a manifestation of what would be a three-dimensional transition if the two-dimensional restriction was removed. Symmetry analysis similar to that of Blackburn *et al.*<sup>29</sup> may help explain why the  $P+S$  wake is seen in two-dimensional flow, whereas the  $2P$  wake is observed when the flow is three-dimensional.

The fact that it is more difficult to generate a  $P+S$  wake at the lower  $Re$  is perhaps not surprising. The stronger diffusion makes it difficult for separate vortical structures of opposite sign to exist without merging, and the higher viscous force makes it harder to split structures in the near wake. Examination of Fig. 2(b) shows that the  $P+S$  mode depends upon a single shed vortex being split by the strain in the near wake, suggesting that viscous suppression of vortex splitting will prevent formation of the  $P+S$  mode until higher strains are experienced at higher amplitudes of oscillation. This viscous suppression seems to be the main governing factor of splitting, at least where  $Re$  is the only variable. Modifying the profile of oscillation to something other

than a sinusoid may introduce other factors, such as the “sharpness” of the change of direction, that could influence the splitting mechanism.<sup>5</sup>

### C. Energy transfer

As well as identifying where the sign of  $C_E$  changes, the value of  $C_E$  anywhere in the synchronization regime is important to establish. This has previously been neglected in the pursuit of identifying the  $C_E=0$  curve. Therefore the presentation of contours of  $C_E$  in the synchronization regime is a novel contribution. It is also important to quantify the correlation between a change in sign of  $C_E$  with a change in the direction of the phase between the lift force and displacement. It has previously been assumed that a sinusoidal oscillation results in a sinusoidal lift force, and therefore that a change in sign of  $C_E$  occurs exactly where there is a change in direction of phase. Both of these issues are addressed in this section.

From many simulations covering parameter space, contours of  $C_E$ , the energy transfer coefficient, have been produced for two values of  $Re$ ,  $Re=100$ , and  $Re=200$ . These contours are shown in Fig. 6. Observation of these contours shows two previously unknown facts. First, the value of  $C_E$  at values of  $A^* < 0.4$  is predominantly determined by the value of frequency, with the contour lines aligned almost vertically, while when  $A^* > 0.4$  the value of  $C_E$  is dictated predominantly by  $A^*$ , with the contours aligned almost horizontally. Secondly, the value of  $C_E$  has no bearing on the wake mode.

That the wake mode is not dependent on  $C_E$  is not surprising when the argument presented in Sec. III B is considered. The changing influence of viscosity with varying  $Re$  means that the amplitude of the transition from one wake mode to the other will differ. This is because a higher strain is required at lower  $Re$  to split the vortex structure in the near wake. For a relatively higher strain, more energy is required, hence increasing the energy transfer from the cylinder to the fluid. Therefore, the transition from  $2S$  to  $P+S$  will not occur at the same  $A^*$  for every  $Re$ .

What this also means is that there may be a change in the direction of energy transfer, a change in the sign of  $C_E$ , with-



FIG. 7. Variation of the wake with increasing amplitude.  $Re=200$ ,  $f/f_{St}=1.01$ ,  $0.2 \leq A^* \leq 0.7$ , increasing in steps of  $\Delta A^*=0.1$ .  $A^*$  increases up the page.  $C_E=0$  is traversed at  $A^* \approx 0.52$ , yet the wake is very similar at  $A^*=0.5$  and  $A^*=0.6$ .

out there being any change in the wake configuration. This is indicative of a delicate balance of interacting forces contributing to the overall lift. By only slightly changing the magnitude of one of these contributing forces, the direction of energy transfer can be reversed. This means the direction of energy transfer is not always simply dependent on the phase of vortex shedding. This fact has been shown previously by Carberry *et al.*<sup>30</sup> for  $Re$  where the flow is three-dimensional.

This effect, where the energy transfer varies but the wake mode shows no significant change, is illustrated in Fig. 7. This figure shows instantaneous wake images for  $Re=200$  and  $f/f_{St}=1.01$ , with the amplitude varying from  $A^*=0.2$  to  $A^*=0.7$ . The direction of energy transfer, or the sign of  $C_E$ , switches at  $A^* \approx 0.52$ ; however, the wakes at  $A^*=0.5$  and  $A^*=0.6$  are very similar, with only a slight change in the distance downstream at which the shed vortices organize themselves into two rows instead of one. All the wakes for  $A^* \leq 0.6$  display the  $2S$  shedding mode, and the



FIG. 8. Variation of the wake with increasing frequency of oscillation.  $Re=200$ ,  $A^*=0.5$ ,  $0.91 \leq f/f_{St} \leq 1.06$ , increasing in steps of  $\Delta f/f_{St}=0.05$ . The frequency,  $f/f_{St}$ , increases up the page.  $C_E=0$  is traversed at  $f/f_{St}=0.95$ , yet no significant change is observed in the wake configuration near this value.

change in sign of  $C_E$  between  $A^*=0.5$  and  $A^*=0.6$  is not correlated with a dramatic change in wake configuration.

Similarly, varying the frequency of oscillation does not see the wake mode vary dramatically, but rather a continuous incremental change occurs with varying frequency. This is shown in Fig. 8. These images are obtained again using  $Re=200$ , but the amplitude is fixed at  $A^*=0.5$  and the frequency of oscillation varied. Again,  $C_E=0$  is traversed, but no significant variation in the wake mode is observed.

The phase of the pressure force, as well as its magnitude, is an important consideration. The phase of the overall pressure force will be dictated by not only the pressure induced by the transverse movement, but also by the position of the shed vortical structures. As the amplitude of oscillation is increased, the position of the forming vortex each half cycle moves further around the back of the cylinder, limiting its effect on the lift force and therefore  $C_E$ . The balance of the forces from the various pressure regions can rapidly alter, leading to a significant change in the phase of the pressure force relative to the displacement.

This change in phase is shown in Fig. 9(a). This shows the effect of the amplitude of oscillation on the phase between the force due to pressure and the transverse displacement, at a fixed  $f/f_{St}=1.0$ , or  $\lambda=5.05$ , where  $\lambda=U/fD$  and  $Re=200$ . Plotted is the phase between the pressure force and displacement, as well as the phase between total force and displacement. At  $A^* \approx 0.5$ , the pressure phase suddenly drops dramatically, taking the overall phase with it. After this drop, the pressure phase stays close to  $-90^\circ$ , the value that would be expected if the pressure was completely determined by

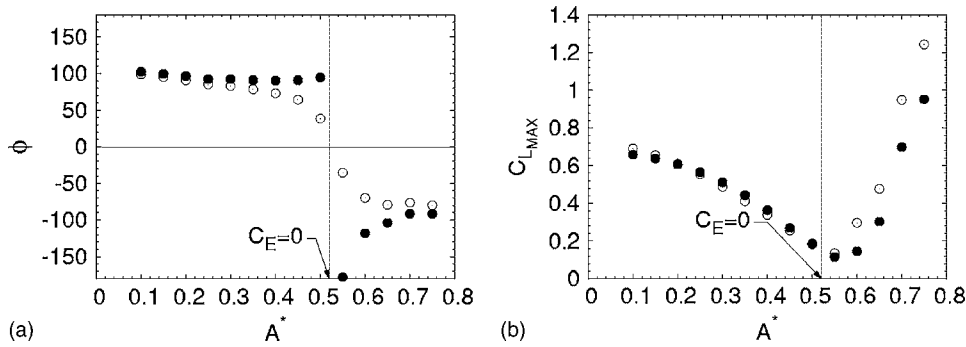


FIG. 9. (a) Phase between lift attributed to pressure and displacement ( $\bullet$ ), and overall lift and displacement ( $\circ$ ), plotted against  $A^*$  for a fixed  $f/f_{Sl} = 1.01$  ( $\lambda = 5.0$ ), for  $Re = 200$ . A sharp change in pressure phase is observed over the range  $0.5 < A^* < 0.6$ , that causes the overall phase to change, and the sign of  $C_E$  to reverse. (b) Maximum lift coefficient of the lift coefficient attributed to pressure ( $\bullet$ ) and overall lift ( $\circ$ ). The minimum of both coincides with the change in phase.

transverse velocity. This dependence on transverse velocity has been observed in higher  $Re$  experiments by Hover *et al.*<sup>9</sup> They plotted contours of lift force in phase with velocity, and found that at amplitudes where  $A^* > 0.6$  these contours were almost horizontal and increasingly negative with increasing  $A^*$ . The concept of this sudden swing in the phase being attributable to the balance between the components changing is supported by Fig. 9(b). Plotted here is the peak lift coefficient magnitude, for both the total lift and the lift due to pressure. It is shown that both are at a minimum at the same amplitude that the phase change occurs at. This minimum is attributable to a vector addition of forces in opposite directions canceling each other. As the minimum is traversed, the dominant vector component changes, which results in a barely noticeable change in magnitude but a sudden change in the direction of force, as observed by the change in phase.

The fact that the overall phase is dictated by this balance of forces implies that there need not be a dramatic change in the phase of vortex shedding for there to be a change in the overall phase. This implication is supported by the evidence presented in Figs. 7 and 8. Even though there is a change in the direction of energy transfer and phase, there is not a significant change in the configuration of the shed vortices. From inspection of Fig. 7 it is clear that the vortex shedding phase can take on any value relative to the displacement. This seems to be different from the behavior observed in higher Reynolds number three-dimensional flow, as it has been reported by Bishop and Hassan,<sup>7</sup> and more recently by Zdravkovich<sup>31</sup> and Carberry *et al.*,<sup>6</sup> where there is a “jump” in the phase of vortex shedding of approximately  $180^\circ$ .

The change in controlling parameter that determines the value of  $C_E$ , from frequency of oscillation at  $A^* < 0.4$ , to an amplitude at  $A^* > 0.4$ , can be explained by considering the forces that are doing work on the cylinder. As the cylinder oscillates only across the stream, only the transverse or lift forces need to be considered in relation to the work done or the energy transferred to or from the cylinder. At high  $A^*$ , the large transverse velocity sees the stagnation point move further around toward the back of the cylinder for a large percentage of the oscillation cycle. This large pressure force, which predominantly scales with velocity, is responsible for the majority of the work done on the cylinder. As this force will be mainly affected by changing the transverse velocity (or, equivalently, changing  $A^*$ ), the work done, or  $C_E$ , will only be significantly changed by changing  $A^*$ .

At lower values of  $A^*$ , the pressure induced by the trans-

verse motion alone is not as great, and does not impose as much control on the lift force and therefore on the energy transfer. The major lift force component in this scenario is from the shed vortices, and the strength of these vortices. In turn, the strength of these vortices is strongly influenced by the acceleration of the cylinder. For a constant oscillation amplitude, the acceleration of the cylinder is proportional to the square of the frequency. This dependence means that at low  $A^*$ ,  $f$  is the dominant parameter determining  $C_E$ .

Further evidence of this balancing of pressure force contributions is apparent from Fig. 10. This shows segments of the lift coefficient time history and instantaneous pressure

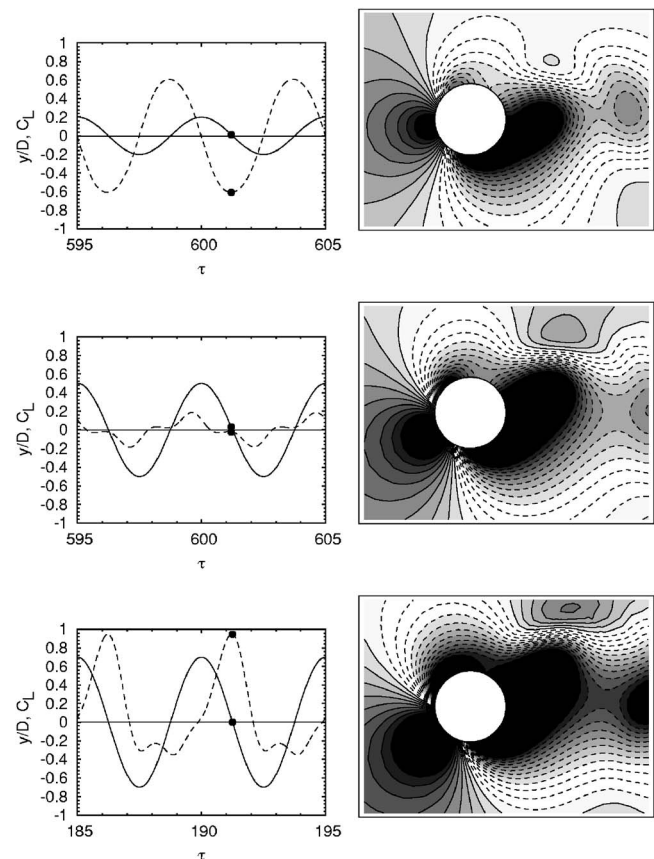


FIG. 10. Lift (- -) and displacement (—) histories, and instantaneous pressure contours, for  $f/f_{Sl} = 1.01$  ( $\lambda = 5.0$ ), (a)  $A^* = 0.20$ , (b)  $A^* = 0.50$ , and (c)  $A^* = 0.70$ ,  $Re = 200$ . Flow is from left to right. The dots on the lift and displacement time history indicate the point in time at which pressure contours are obtained. Negative contour levels are indicated with dotted lines.

contours for  $f/f_{St}=1.01$  and  $A^*=0.2, 0.5, 0.7$ . For  $A^*=0.2$ , shown in Fig. 10(a), the lift time history is sinusoidal, with the lift coefficient,  $C_L$ , leading  $y/D$ . The pressure contours, taken close to an instant where  $y/D=0$  (at maximum transverse velocity) show the stagnation point is near the front of the cylinder, and the large negative pressure region of the forming vortex centered near the immediate rear of the cylinder.

When  $A^*=0.5$ , the lift history shows a large deviation from a pure sinusoid, as shown in Fig. 10(b). This deviation is most likely caused by the reorganization of significant pressure regions (stagnation point, forming, and shed vortices) with relation to the oscillation cycle, and each other. At  $A^*=0.5$ , it is shown that the overall magnitude of the lift force has been significantly reduced compared to the lower amplitude case.

Further increasing  $A^*$  to  $A^*=0.7$  sees the wake mode change to  $P+S$ , with a corresponding marked change in the lift force history, as shown in Fig. 10(c). The asymmetry of the wake is reflected in the nonzero mean lift, and the lift force variation over the oscillation cycle is far from sinusoidal. The pressure contours show that the stagnation point has moved further towards the back of the cylinder. It is hypothesized that it is the combination of this high pressure, now oriented such that its major influence is on the total lift force, with the single vortex shed in one half-cycle of oscillation that causes the high-magnitude peak seen in the lift trace.

#### IV. CONCLUSIONS

Two detailed maps of the observed wake modes in frequency-amplitude space have been produced for two different values of  $Re$ . Two new and important conclusions can be drawn from these maps. First, the synchronization regime and the wake modes observed within the synchronized regime are expressly shown to be  $Re$  dependent. This dependence is consistent with the proportionally higher viscous forces at lower  $Re$ . Second, a comparison of these maps with the wake map of Williamson and Roshko,<sup>3</sup> where the flow is three-dimensional indicates that the wake modes are dependent on flow dimensionality, with different wake modes observed during the current study compared to those reported in that study. Further evidence that this result is governed by dimension, and not simply  $Re$ , is found in Blackburn and Henderson,<sup>8</sup> where two-dimensional simulations were performed at Reynolds numbers where the flow would normally be three-dimensional, and wake modes similar to those of the current study were observed.

The energy transfer characteristics throughout the synchronization region have also been quantified. It is found that regardless of  $Re$ , the energy transfer is mainly dependent on frequency at lower amplitudes, but becomes primarily dependent on amplitude as the amplitude is increased. A explanation for this is the changing dominance of the force due to the stagnation pressure and the force due to the pressure induced by the vortices shed into the wake.

The upper limit of the zero energy transfer contour is found to be at  $A^*\approx 0.6$ , regardless of  $Re$ . This agrees well

with the highest amplitudes observed in two-dimensional vortex-induced vibration of elastically mounted cylinders.<sup>24</sup> However, showing that this limit is independent of  $Re$  is a new result. It is also interesting that this limit is independent of  $Re$  whereas the wake mode boundaries are not.

Comparison of the boundary defining the transition from the  $2S$  to  $P+S$  wake mode with the energy transfer contours expressly demonstrates that the wake mode obtained is not dependent on the value of  $C_E$ . This is not surprising considering the dependence of this transition on  $Re$ . However, as the sign of  $C_E$  is very closely linked to the direction of the phase between the lift and displacement, it does show that a swing in this phase does not necessarily result in a swing in the phase of vortex shedding. In fact, the change in flow structure is shown to be virtually nonexistent, with no visible change occurring in the wake structure. It has also been shown that the transition from  $2S$  to  $P+S$  shedding is not dependent even on the direction of energy transfer, in agreement with the single  $Re$ , single amplitude implication of Blackburn and Henderson.<sup>8</sup> This lack of correlation between  $C_E$  and wake mode also indicates that a change in the sign of  $C_E$ , and hence the direction of energy transfer, can occur without any significant change being observed in the wake mode. This is further confirmed by the  $Re$  dependence of the  $2S$  to  $P+S$  transition demonstrated herein.

#### ACKNOWLEDGMENTS

J.L. would like to acknowledge the financial support provided through a Monash Departmental Scholarship. The authors would like to acknowledge the strong support offered from the Victorian Partnership for Advanced Computing and the Australian Partnership for Advanced Computing, that enabled this study to take place.

- <sup>1</sup>T. Sarpkaya, "A critical review of the intrinsic nature of vortex-induced vibrations," *J. Fluids Struct.* **19**, 389 (2004).
- <sup>2</sup>C. H. K. Williamson and R. Govardhan, "Vortex-induced vibrations," *Annu. Rev. Fluid Mech.* **36**, 413 (2004).
- <sup>3</sup>C. H. K. Williamson and A. Roshko, "Vortex formation in the wake of an oscillating cylinder," *J. Fluids Struct.* **2**, 355 (1988).
- <sup>4</sup>R. Govardhan and C. H. K. Williamson, "Modes of vortex formation and frequency response of a freely vibrating cylinder," *J. Fluid Mech.* **420**, 85 (2000).
- <sup>5</sup>F. L. Ponta and H. Aref, "Vortex synchronization regions in shedding from an oscillating cylinder," *Phys. Fluids* **17**, 011703 (2005).
- <sup>6</sup>J. Carberry, J. Sheridan, and D. Rockwell, "Forces and wake modes of an oscillating cylinder," *J. Fluids Struct.* **15**, 523 (2001).
- <sup>7</sup>R. E. D. Bishop and A. Y. Hassan, "The lift and drag forces on a circular cylinder oscillating in a flowing fluid," *Proc. R. Soc. London, Ser. A* **277**, 51 (1964).
- <sup>8</sup>H. M. Blackburn and R. Henderson, "A study of two-dimensional flow past an oscillating cylinder," *J. Fluid Mech.* **1385**, 255 (1999).
- <sup>9</sup>F. S. Hover, A. H. Techet, and M. S. Triantafyllou, "Forces on oscillating uniform and tapered cylinders in crossflow," *J. Fluid Mech.* **363**, 97 (1998).
- <sup>10</sup>X.-Y. Lu and C. Dalton, "Calculating of the timing of vortex formation from an oscillating cylinder," *J. Fluids Struct.* **10**, 527 (1996).
- <sup>11</sup>J. R. Meneghini and P. W. Bearman, "Numerical simulation of high amplitude oscillatory flow about a circular cylinder," *J. Fluids Struct.* **9**, 435 (1995).
- <sup>12</sup>T. Staubli, "Calculation of the vibration of an elastically mounted cylinder using experimental data from forced oscillation," *J. Fluids Eng.* **105**, 225 (1983).
- <sup>13</sup>O. M. Griffin, "The unsteady wake of an oscillating cylinder at low Reynolds number," *J. Appl. Mech.* **38**, 729 (1971).

- <sup>14</sup>G. H. Koopman, "The vortex wakes of vibrating cylinders at low Reynolds numbers," *J. Fluid Mech.* **28**, 501 (1967).
- <sup>15</sup>G. E. Karniadakis, M. Israeli, and S. A. Orszag, "High-order splitting methods of the incompressible Navier-Stokes equations," *J. Comput. Phys.* **97**, 414 (1991).
- <sup>16</sup>M. C. Thompson, K. Hourigan, and J. Sheridan, "Three-dimensional instabilities in the wake of a circular cylinder," *Exp. Therm. Fluid Sci.* **12**, 190 (1996).
- <sup>17</sup>K. Ryan, M. C. Thompson, and K. Hourigan, "Three-dimensional transition in the wake of bluff elongated cylinders," *J. Fluid Mech.* **538**, 1 (2005).
- <sup>18</sup>M. C. Thompson, T. Leweke, and C. H. K. Williamson, "The physical mechanism of transition in bluff body wakes," *J. Fluids Struct.* **15**, 607 (2001).
- <sup>19</sup>M. C. Thompson, T. Leweke, and M. Provansal, "Kinematics and dynamics of sphere wake transition," *J. Fluids Struct.* **15**, 575 (2001).
- <sup>20</sup>G. Sheard, M. C. Thompson, and K. Hourigan, "From spheres to circular cylinders: the stability and flow structures of bluff ring wakes," *J. Fluid Mech.* **492**, 147 (2003).
- <sup>21</sup>K. Hourigan, M. C. Thompson, and B. T. Tan, "Self-sustained oscillations in flows around long flat plates," *J. Fluids Struct.* **15**, 387 (2001).
- <sup>22</sup>J. R. Meneghini and P. W. Bearman, Numerical simulation of high amplitude oscillatory flow about a circular cylinder using a discrete vortex method, in *Shear Flow Conference AIAA Pap.* 93-3288, Orlando, FL, Jul. 6-9, 1993.
- <sup>23</sup>E. Berger, "Suppression of vortex shedding and turbulence behind oscillating cylinders," *Phys. Fluids* **10**, S191 (1967).
- <sup>24</sup>P. Anagnostopoulos and P. W. Bearman, "Response characteristics of a vortex-excited cylinder at low Reynolds numbers," *J. Fluids Struct.* **6**, 39 (1992).
- <sup>25</sup>H. M. Blackburn and R. Henderson, "Lock-in behavior in simulated vortex-induced vibration," *Exp. Fluids* **12**, 184 (1996).
- <sup>26</sup>G. Iooss and D. D. Joseph, *Elementary Stability and Bifurcation Theory* (Springer-Verlag, New York, 1990).
- <sup>27</sup>H. M. Blackburn and J. M. Lopez, "On three-dimensional quasiperiodic Floquet instabilities of two-dimensional bluff body wakes," *Phys. Fluids* **15**, L57 (2003).
- <sup>28</sup>F. Marques, J. M. Lopez, and H. M. Blackburn, "Bifurcations in systems with  $Z_2$  spatio-temporal and  $O(2)$  spatial symmetry," *Physica D* **189**, 247 (2004).
- <sup>29</sup>H. M. Blackburn, F. Marques, and J. M. Lopez, "Symmetry breaking of two-dimensional time-periodic wakes," *J. Fluid Mech.* **522**, 395 (2005).
- <sup>30</sup>J. Carberry, J. Sheridan, and D. Rockwell, "Controlled oscillations of a cylinder: A new wake state," *J. Fluids Struct.* **17**, 337 (2003).
- <sup>31</sup>M. M. Zdravkovich, "Modification of vortex shedding in the synchronization range," *J. Fluids Eng.* **104**, 513 (1982).